

## Surface tension effect on the mechanical properties of nanomaterials measured by atomic force microscopy

Stéphane Cuenot,<sup>1</sup> Christian Frétygny,<sup>2</sup> Sophie Demoustier-Champagne,<sup>1</sup> and Bernard Nysten,<sup>1,\*</sup><sup>1</sup>*Unité de chimie et de physique des hauts polymères & Research Center on Micro- and Nanoscopic Materials and Electronic Devices, Université Catholique de Louvain, Croix du Sud, 1, B-1348 Louvain-la-Neuve, Belgium*<sup>2</sup>*Physico-Chimie Structurale et Macromoléculaire, CNRS UMR 7615, ESPCI, 10 rue Vauquelin, F-75231 Paris Cedex 05, France*

(Received 20 August 2003; revised manuscript received 28 January 2004; published 20 April 2004)

The effect of reduced size on the elastic properties measured on silver and lead nanowires and on polypyrrole nanotubes with an outer diameter ranging between 30 and 250 nm is presented and discussed. Resonant-contact atomic force microscopy (AFM) is used to measure their apparent elastic modulus. The measured modulus of the nanomaterials with smaller diameters is significantly higher than that of the larger ones. The latter is comparable to the macroscopic modulus of the materials. The increase of the apparent elastic modulus for the smaller diameters is attributed to surface tension effects. The surface tension of the probed material may be experimentally determined from these AFM measurements.

DOI: 10.1103/PhysRevB.69.165410

PACS number(s): 81.07.-b, 62.25.+g, 07.79.Lh

Materials with reduced size and dimensionality such as thin films, nanowires, nanotubes, or metallic clusters may present exceptional properties compared to those of the corresponding macroscopic materials. Thanks to these particular properties, these materials have given rise to a much interest. Nanomaterials present many different challenges due to their small size such as their manipulation or the measurement of their physical properties. The developments of scanning probe microscopies (SPM's) allowed the emergence of new powerful means for material characterization at the microscale and nanoscale. Especially, atomic force microscopy (AFM) is widely used to study material<sup>1-4</sup> as well as nanostructure mechanical properties.<sup>5-8</sup>

The mechanical behavior of materials at the nanoscale is often different from that at macroscopic scale. Though continuum mechanics applies when sizes are above the 10-nm range, surface effects may control the deformation properties. For structures with micrometer sizes, the mechanical properties are controlled by the elastic strain energy. At nanometer length scales, due to the increasing surface-to-volume ratio, surface effects become predominant and can significantly modify the macroscopic properties. Although some authors recognized that surface effects could play a major role in the measured properties,<sup>9-11</sup> few experimental results exist concerning the influence of reduced size on the mechanical properties. Some authors have already proposed to include surface contributions through a gradient elasticity approach.<sup>12,13</sup> Cammarata clearly distinguishes surface tension and surface energy concepts, which are often misunderstood, and describes the effect of surface tension on the mechanical properties of thin films.<sup>14</sup> From experimental results obtained on organic and inorganic nanomaterials, the present paper analyzes the size effects on the mechanical properties.

Electrostatic resonant-contact AFM was used to determine the Young's modulus of nanotubes and nanowires. This method allows the excitation of the cantilever vibration without any modification of it and does not present the classical drawbacks and limitations of tapping mode, force modulation, and force-curve measurements.<sup>15,16</sup> A sinusoidal external electric field applied between the sample holder and mi-

croscope head induces the cantilever vibration. By varying the frequency of the electric field, the resonance spectrum of cantilevers can be fully characterized while the tip contacts the sample surface or not. When the tip is in contact with the sample, the cantilever resonance frequencies shift to higher values relatively to those of the free cantilever. Several studies demonstrated that the resonance frequency of a cantilever in contact with a surface strongly depends on the contact stiffness.<sup>2,17-20</sup> The resonance frequency of a cantilever with the tip in contact with a sample can thus be used to measure the local stiffness, if the "tip-surface" contact is correctly modeled. In the present experiments, the overall deformation of the structures rather than contact deformation is responsible for the observed shifts and elastic modulus of the nanostructures can be quantitatively determined.<sup>16</sup>

Metallic wires and polymer tubes were synthesized using a template-based method within the pores of polycarbonate (PC) track-etched membranes.<sup>21</sup> Silver and lead nanowires were electrochemically synthesized from solutions containing respectively AgNO<sub>3</sub> and Pb(BF<sub>4</sub>)<sub>2</sub>. Nanotubes of a conductive polymers [polypyrrole (PPy)] were electrochemically synthesized using the procedure extensively described elsewhere.<sup>6,21</sup> To obtain nanomaterials with different outer diameters, 20- $\mu$ m-thick membranes with pore size ranging between 30 and 250 nm were used. For such diameters, continuum mechanics models are expected to remain valid.

After synthesis, the membrane was dissolved by immersion in a dichloromethane solution containing dodecyl sulfate as surfactant<sup>22</sup> and the suspension was placed in an ultrasonic bath during 1 h to separate the nanostructures from the gold film previously evaporated on the backside of the membrane. The suspensions were then filtered through poly(ethylene terephthalate) (PET) membranes with pore diameters ranging between 0.8 and 3  $\mu$ m. In order to remove any contaminant from the nanomaterial surface the samples were thoroughly rinsed with dichloromethane. To minimize shear deformations in the experiment, the ratio between the suspended length of the tube or beam,  $L$ , and its outer diameter  $D$  should be higher than 16 (Ref. 23). To achieve this, each series of nanowires or nanotubes synthesized in a template

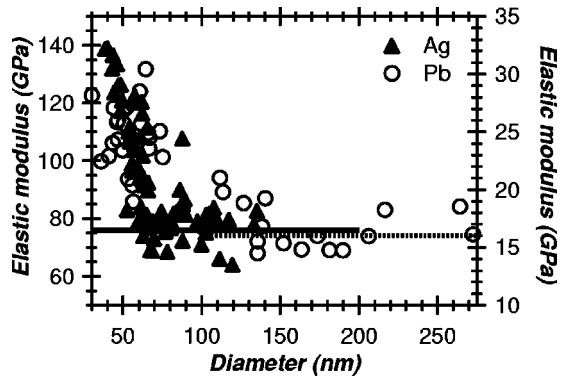


FIG. 1. Variation of the measured elastic modulus for Ag (left scale) and Pb (right scale) nanowires as a function of the diameter. The solid line corresponds to the elastic modulus of bulk silver and the dotted line to the elastic modulus of bulk Pb.

membrane with a specific pore diameter was dispersed on a corresponding PET membrane with a pore diameter satisfying this criterion.

The AFM experiments were performed with an Autoprobe CP (Thermomicroscopes) operated in air with a 100- $\mu\text{m}$  scanner equipped with ScanMaster detectors correcting for nonlinearity and hysteresis effects. The cantilevers were standard  $\text{Si}_3\text{N}_4$  Microlevers with integrated pyramidal tips (typical apex radius of curvature between 30 and 50 nm) and with free resonance frequencies around 100 kHz. The modulated electric field was applied between the sample holder and AFM head using a function generator (Agilent Technologies, model 33120A). In order to avoid tip displacement on the sample surface and to keep resonance peak symmetrical,<sup>24</sup> resonance spectra were recorded with small peak-to-peak excitation amplitude.<sup>15</sup> The cantilever deflection signal was measured using a lock-in amplifier (EG&G Princeton Applied Research, model S302). The signal generator command and the data collection from the lock-in amplifier were computerized and data analysis was realized using Igor Pro software (Wavemetrics).

Large-scale images were first acquired to select nanomaterials suspended over pores. Then an image at lower scale was realized to determine the nanostructure dimensions—i.e.,  $L$  and  $D$ . Here  $D$  was determined by measurement of the height relatively to the supporting membrane to avoid tip artifacts. The inner diameter  $D_{\text{in}}$  of the PPy nanotubes was estimated using a previously established calibration curve relating the outer and inner diameters.<sup>6</sup>

The AFM tip was then located at the midpoint along the suspended length and resonance spectrum of the cantilever in contact with the nanowire or nanotube was measured. Before each measurement, the normal force applied by the cantilever was canceled by zeroing its vertical deflection so that only adhesion and electrostatic forces were applied. The measurements were performed on series of Ag and Pb nanowires and PPy nanotubes with diameter ranging from 30 to 250 nm. The elastic modulus was deduced from the measured nanotube stiffness as described elsewhere.<sup>16</sup>

In Fig. 1, the measured values of the elastic modulus of Ag and Pb nanowires are reported as a function of the diam-

eter. For large diameters ( $>70$  nm for Ag,  $>100$  nm for Pb), the measured values are almost independent of the diameter and are close to the values reported in the literature for the bulk materials—i.e., 76 GPa for Ag (Ref. 25) and 16 GPa for Pb (Ref. 26). When  $D$  decreases down to 30 nm, the measured elastic modulus continuously increases. The same behavior was previously observed for PPy nanotubes.<sup>6,16</sup> For the metallic nanowires with the smallest diameters, the measured modulus is approximately twice the Young's modulus of bulk materials (around 140 GPa for Ag and 30 GPa for Pb). For the PPy nanotubes, the effect is even more pronounced. The measured modulus increased by more than one order of magnitude to reach a value about 120 GPa for  $D$  around 35 nm (Ref. 16).

Such an increase may originate from structural modifications of the materials for the smaller diameters, though the elastic modulus is known to be rather insensitive to the defect concentration. Several reasons indicate that this could not be the case. First, we verified that the same modulus values were obtained for PPy samples synthesized at two different temperatures ( $-10$  and  $20^\circ\text{C}$ ). Indeed, it was previously showed that the electrical conductivity of PPy nanotubes synthesized at lower temperature increases compared to that of those synthesized at room temperature.<sup>27</sup> This increase was attributed to a better alignment and a better structural perfection of the polymer chains. The fact that we did not observe any effect of the synthesis temperature for the elastic modulus may rule out this explanation for this latter property. Moreover, AFM images show that the diameters are very constant along the rods and that their surface is smooth. Therefore the size of the defects is expected to be small compared to the tube diameter. Finally, transmission electron microscopy did not reveal any structural modification between the smallest and largest nanotubes or nanowires.

As deformation of the beam induces an increase of its area, surface tension effects may also account for the observed results. Therefore, a calculation of the stiffness of the suspended nanotubes due to the elastic modulus and surface tension is proposed. As the magnitude of the nanostructure deflection was always small compared to its diameter, the theory of small deflections of beams is applied to evaluate the contribution of surface effects on the nanostructure stiffness.<sup>28</sup> The boundary conditions of the suspended nanowires and nanotubes were previously determined<sup>16</sup> and correspond to those of clamped-ends beams. Assuming a force  $F$  applied at the beam midpoint and inducing a deflection  $\delta$ , an expression for the total energy  $U$  of the bent beam is

$$U = -F\delta + \frac{1}{2}k_t\delta^2 + \gamma\Phi\Delta L(1-\nu), \quad (1)$$

where  $k_t$  is the beam elastic stiffness,  $\Phi$  is the contour length of its section,  $\Delta L$  its length variation,  $\nu$  is the Poisson's ratio, and  $\gamma$  is the surface tension of the material. For these clamped conditions, the elastic stiffness is<sup>28</sup>

$$k_t = \frac{192EI}{L^3}, \quad (2)$$

where  $E$  is the material Young's modulus and  $I$  the moment of inertia of the section. In relation (1), the first term is the work of the applied force, the second one represents the elastic deformation energy of the bent beam, and the third one corresponds to the deformation energy of the surface resulting from beam extension. The bending of a beam with both ends clamped, so that no longitudinal displacement at the ends is possible, results in an extension of its length and, hence, in an increase of the surface. The energy term dealing with the surface increase takes into account the compressibility  $\nu$  of the material. For slight bending, the extension of the bent beam is given by

$$\Delta L = \frac{1}{2} \int_0^L y'(x)^2 dx, \quad (3)$$

where  $y(x)$  is the deflection curve of the beam with a concentrated load applied at the midpoint of the suspended length.<sup>28</sup> Due to linearity, the surface deformation energy term has a quadratic dependence on the central deflection, giving rise to an additive surface contribution to the beam stiffness. As a first approximation, it is assumed that the usual deflection curve of a clamped beam is not affected by the surface tension contribution. For clamped boundary conditions, the beam extension can be easily calculated and expressed as

$$\Delta L = \frac{12}{5} \frac{\delta^2}{L}. \quad (4)$$

Introducing relation (4) into relation (1), the following expression for the total energy of the bent beam is obtained:

$$U = -F\delta + \frac{1}{2}(k_t + k_s)\delta^2, \quad (5)$$

where

$$k_s = \frac{24}{5} \gamma \frac{\Phi}{L} (1 - \nu).$$

From the equilibrium condition, an apparent stiffness of the beam,  $k_{app}$ , can be defined:

$$k_{app} = k_t + k_s. \quad (6)$$

If the apparent stiffness is interpreted as only due to elastic properties of the material, an apparent elastic modulus can be deduced from the measured stiffness as was assumed in Fig. 1 to interpret the experimental data:

$$E_{app} \equiv \frac{L^3}{192I} k_{app} = E + \frac{1}{40} \gamma (1 - \nu) \Phi \frac{L^2}{I}. \quad (7)$$

For nanowires,  $\Phi = \pi D$  and  $I = \pi D^4/64$ . Expressions (6) and (7) become

$$k_{app} = 3\pi \frac{D^4}{L^3} E + \frac{24\pi}{5} \gamma (1 - \nu) \frac{D}{L}, \quad (8)$$

$$E_{app} = E + \frac{8}{5} \gamma (1 - \nu) \frac{L^2}{D^3}. \quad (9)$$

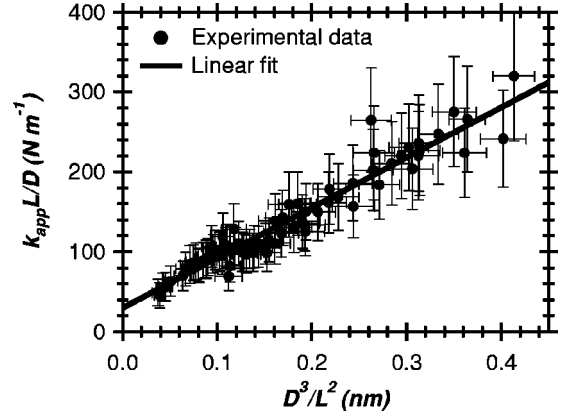


FIG. 2. Product of the apparent stiffness and  $L/D$  of Ag nanowires as a function of  $D^3/L^2$ . The solid line represents the fit of the experimental data (●) based on relation (8).

From Eq. (8), reporting the apparent stiffness multiplied by  $L/D$  versus the geometrical parameter  $D^3/L^2$  should give a linear relation. A nonzero intercept with the ordinate axis is expected to be due to the surface tension contribution. This is shown in Fig. 2 for the Ag nanowires. Linear regression allows the determination of the elastic modulus and surface tension. For Ag, the so-obtained elastic modulus is equal to  $67.5 \pm 2.1$  GPa comparable to the value of the modulus of silver [76 GPa (Ref. 25)]. The same analysis of the results on the Pb nanowires leads to a value of  $16.9 \pm 0.8$  GPa comparable to the modulus of Pb [16 GPa (Ref. 26)]. The regressions give also access to the surface tension of the probed materials knowing their Poisson's ratio. The value of the surface tension for the Ag nanowires was of  $3.09 \pm 0.33$  J m<sup>-2</sup>, determined with a Poisson's ratio of 0.37 (Ref. 29). For the Pb nanowires, a value of  $0.98 \pm 0.21$  J m<sup>-2</sup> was obtained using a Poisson's ratio of 0.42 (Ref. 30).

In the case of nanotubes, the apparent stiffness and tensile modulus are given by the expressions

$$k_{app} = 3\pi E \frac{D^4 - D_{in}^4}{L^3} + \frac{24}{5} \pi \gamma (1 - \nu) \frac{D + D_{in}}{L}, \quad (10)$$

$$E_{app} = E + \frac{8}{5} \gamma (1 - \nu) L^2 \frac{D + D_{in}}{D^4 - D_{in}^4}. \quad (11)$$

Using relation (10), the fit of the experimental data from Ref. 16 gives a value of  $0.6 \pm 0.3$  GPa for the elastic modulus of PPy. With a typical value of the Poisson's ratio for polymers of 0.4 (Ref. 31), a value of  $0.33 \pm 0.01$  J m<sup>-2</sup> is determined for the surface tension. The obtained value for the modulus is comparable to that reported in the literature for PPy films though somehow lower (1.2 and 3.2 GPa for PPy films).<sup>32,33</sup>

In contrast to liquids, surface energy and surface tension refer to two different concepts in the case of solids, which are often misunderstood.<sup>14,34</sup> Surface energy is defined as the reversible work per unit area needed to create a new surface. On the other hand, surface tension or surface stress is the reversible work per unit area needed to elastically stretch a preexisting surface. In our AFM experiments, as the sus-

pendent nanomaterials are deformed, the surface tension is solicited. It should be noted that there are very few experimental measurements of surface tension and most values reported in the literature arise from theoretical calculations. These calculations predict that surface tension values are of the same order of magnitude and slightly higher than the surface energy values.<sup>14</sup>

Wassermann and Vermaak have experimentally determined the surface tension value for silver from the measurement of the lattice contraction in small Ag spheres as a function of their radius by electron diffraction.<sup>35</sup> The obtained value for the surface tension was equal to  $1.41 \pm 0.30 \text{ J m}^{-2}$  at  $55^\circ\text{C}$ . This value is similar to the present result ( $3.09 \pm 0.33 \text{ J m}^{-2}$ ). To our knowledge, no data are available for the surface tension of Pb and PPy. It can, however, be noticed that the obtained surface tension values ( $0.98 \pm 0.21$  and  $0.33 \pm 0.01 \text{ J m}^{-2}$ , respectively, for Pb and PPy) are comparable to published values of the surface energy [between  $0.5$  and  $0.6 \text{ J m}^{-2}$  for Pb (Ref. 36) and  $0.145 \text{ J m}^{-2}$  for PPyCl (Ref. 37) films].

From relations (2) and (5), it is possible to derive a ratio that could be used to predict the onset of the surface tension effects. For nanowires, this ratio between the surface stiffness  $k_s$  and tensile stiffness  $k_t$  can be expressed as

$$\frac{k_s}{k_t} = \frac{8}{5} \frac{\gamma}{E} \frac{L^2}{D^3} (1 - \nu). \quad (12)$$

When this ratio is larger than 1, surface tension effects prevail. It is important to notice the dependence of this ratio on the geometrical dimensions of the probed nanostructure. Depending on the suspended length, surface effects may arise for different diameters. Moreover, this ratio is established for a specific geometry of solicitation (clamped ends, central solicitation) and therefore it is not an intrinsic material quantity. In others tests, surface tension effects could show up for different geometrical conditions. We can, how-

ever, expect that only small numerical factors will modify this ratio, leading to comparable geometrical effects.

The ratio between the apparent elastic modulus of the smallest nanomaterial and the corresponding macroscopic modulus of the material is much larger for the PPy nanotubes than for the metallic nanowires. In both cases, surface effects explain the increase of the apparent elastic modulus. The larger effect in the case of PPy nanotubes is essentially due to the intrinsic lower elastic modulus of the material rather than to the additional inner surface existing in nanotubes. Though defect concentration effects cannot be ruled out to explain the apparent modulus increase observed in our experimental data, we suggest that surface tension is mainly responsible for the observed increase.

In conclusion, the elastic modulus of metallic nanowires and polymer nanotubes with diameters ranging between 30 and 250 nm was measured using resonant-contact AFM. For the smaller diameters, the measured elastic modulus significantly differs from that of the bulk materials. Calculation of an apparent elastic modulus taking into account the surface effect shows that the observed increase of the elastic modulus with decreasing diameter is essentially due to surface tension effects. This model allows the calculation of the intrinsic elastic modulus and the surface tension of the probed material from the measured apparent modulus. For Ag nanowires a fairly good agreement is obtained with the values published in the literature. In summary, we showed that, in the case of metallic nanowires and polymer nanotubes, the increase of the surface to volume ratio with decreasing size strongly influences the measured modulus and that AFM measurements of it enables the evaluation of solid surface tension.

The authors gratefully acknowledge Dr. J.-P. Aimé and Professor D. Johnson for invaluable discussions. They acknowledge the FRFC and IUAP-V-P03/11 program for financial support. S.C. was financially supported by the FSR of the UCL. B.N. and S.D.C. are supported by the FNRS.

\*Corresponding author. Electronic address: nysten@poly.ucl.ac.be

<sup>1</sup>C. Basire and C. Frétygny, *Eur. Phys. J.: Appl. Phys.* **6**, 323 (1999).

<sup>2</sup>F. Dinelli, S. K. Biswas, G. A. D. Briggs, and O. V. Kolosov, *Phys. Rev. B* **61**, 13 995 (2000).

<sup>3</sup>E. Tomasetti, R. Legras, and B. Nysten, *Nanotechnology* **9**, 305 (1998).

<sup>4</sup>F. Oulevey, G. Gremaud, A. Semoroz, A. J. Kulik, N. A. Burnham, E. Dupas, and D. Gourdon, *Rev. Sci. Instrum.* **69**, 2085 (1998).

<sup>5</sup>J.-P. Salvétat, G. A. D. Briggs, J.-M. Bonard, R. R. Bacsá, A. J. Kulik, T. Stöckli, N. A. Burnham, and L. Forro, *Phys. Rev. Lett.* **82**, 944 (1999).

<sup>6</sup>S. Cuenot, S. Demoustier-Champagne, and B. Nysten, *Phys. Rev. Lett.* **85**, 1690 (2000).

<sup>7</sup>M.-F. Yu, O. Lourie, M. J. Dyer, K. Moloni, T. F. Kelly, and R. S. Ruoff, *Science* **287**, 637 (2000).

<sup>8</sup>P. Poncharal, Z. L. Wang, D. Ugarte, and W. A. de Heer, *Science* **283**, 1513 (1999).

<sup>9</sup>M. E. Gurtin and A. Murdoch, *Arch. Ration. Mech. Anal.* **57**, 291 (1975).

<sup>10</sup>R. E. Miller and V. B. Shenoy, *Nanotechnology* **11**, 139 (2000).

<sup>11</sup>P. Sharma, S. Ganti, and N. Bhate, *Appl. Phys. Lett.* **82**, 535 (2003).

<sup>12</sup>B. S. Altan, H. A. Evensen, and E. C. Aifantis, *Mech. Res. Commun.* **23**, 35 (1996).

<sup>13</sup>S. Papargyri-Beskou, K. G. Tsepoura, D. Polyzos, and D. E. Beskos, *Int. J. Solids Struct.* **40**, 385 (2003).

<sup>14</sup>R. C. Cammarata, *Prog. Surf. Sci.* **46**, 1 (1994).

<sup>15</sup>C. Frétygny (unpublished).

<sup>16</sup>S. Cuenot, C. Frétygny, S. Demoustier-Champagne, and B. Nysten, *J. Appl. Phys.* **93**, 5650 (2003).

<sup>17</sup>K. Yamanaka, H. Ogiso, and O. V. Kolosov, *Appl. Phys. Lett.* **64**, 178 (1994).

<sup>18</sup>K. Yamanaka and S. Nakano, *Appl. Phys. A: Mater. Sci. Process.* **66**, S313 (1998).

<sup>19</sup>P. Vairac and B. Cretin, *Surf. Interface Anal.* **27**, 588 (1999).

<sup>20</sup>U. Rabe, K. Janser, and W. Arnold, *Rev. Sci. Instrum.* **67**, 3281 (1996).

<sup>21</sup>S. Demoustier-Champagne and P.-Y. Stavaux, *Chem. Mater.* **11**, 829 (1999).

- <sup>22</sup>S. De Vito and C. R. Martin, *Chem. Mater.* **10**, 1738 (1998).
- <sup>23</sup>S. P. Timoshenko and J. M. Gere, *Mechanics of Materials* (Van Nostrand, New York, 1972).
- <sup>24</sup>U. Rabe, E. Kester, and W. Arnold, *Surf. Interface Anal.* **27**, 386 (1999).
- <sup>25</sup>M. F. Ashby and D. R. H. Jones, *Engineering Materials* (Pergamon, Oxford, 1980), Vol. 1.
- <sup>26</sup>N. E. Dowling, *Mechanical Behavior of Materials: Engineering Methods for Deformation, Fracture, and Fatigue* (Prentice Hall, Upper Saddle River, NJ, 1999).
- <sup>27</sup>C. R. Martin, *Science* **266**, 1961 (1994).
- <sup>28</sup>L. D. Landau and E. M. Lifshitz, *Theory of Elasticity* (Pergamon, Oxford, 1970).
- <sup>29</sup>G. Perrin, *J. Phys. Chem. Solids* **62**, 2091 (2001).
- <sup>30</sup>A. M. James and M. P. Lord, *Chemical and Physical Data* (Macmillan, London, 1992).
- <sup>31</sup>J. Brandrup and E. H. Immergut, *Polymer Handbook*, 3rd ed. (Wiley, New York, 1989).
- <sup>32</sup>B. Sun, J. J. Jones, R. P. Burford, and M. Skyllas-Kazacos, *J. Mater. Sci.* **24**, 4024 (1989).
- <sup>33</sup>M. Gandhi, G. M. Spinks, R. P. Burford, and G. G. Wallace, *Polymer* **36**, 4761 (1995).
- <sup>34</sup>J. W. Gibbs, *The Scientific Papers of J. W. Gibbs* (Longmans-Green, London, 1906) Vol. 1.
- <sup>35</sup>H. J. Wassermann and J. S. Vermaak, *Surf. Sci.* **22**, 164 (1970).
- <sup>36</sup>M. Mansfield and R. J. Needs, *Phys. Rev. B* **43**, 8829 (1991).
- <sup>37</sup>M. M. Chehimi, M.-L. Abel, C. Perruchot, M. Delamar, S. F. Lascelles, and S. P. Armes, *Synth. Met.* **104**, 51 (1999).